Europace (2016) **18**, iv136–iv145
doi:10.1093/europace/euw358

SUPPLEMENT PAPER

Towards personalized computational modelling of the fibrotic substrate for atrial arrhythmia

Patrick M. Boyle, Sohail Zahid, and Natalia A. Trayanova*

Department of Biomedical Engineering and Institute for Computational Medicine, Johns Hopkins University, 3400 N Charles St, 208 Hackerman Hall, Baltimore, MD 21218, USA

Received 8 April 2016; accepted after revision 28 July 2016

Atrial arrhythmias involving a fibrotic substrate are an important cause of morbidity and mortality. In many cases, effective treatment of such rhythm disorders is severely hindered by a lack of mechanistic understanding relating features of fibrotic remodelling to dynamics of re-entrant arrhythmia. With the advent of clinical imaging modalities capable of resolving the unique fibrosis spatial pattern present in the atria of each individual patient, a promising new research trajectory has emerged in which personalized computational models are used to analyse mechanistic underpinnings of arrhythmia dynamics based on the distribution of fibrotic tissue. In this review, we first present findings that have yielded a robust and detailed biophysical representation of fibrotic substrate electrophysiological properties. Then, we summarize the results of several recent investigations seeking to use organ-scale models of the fibrotic human atria to derive new insights on mechanisms of arrhythmia perpetuation and to develop novel strategies for model-assisted individualized planning of catheter ablation procedures for atrial arrhythmias.

Keywords Atrial fibrillation • Atrial flutter • Computational modelling • Fibrotic remodelling

Introduction

Atrial arrhythmias that involve fibrotic substrates are increasingly prevalent and extremely difficult to treat. Atrial fibrillation (AF) is the most common cardiac arrhythmia and a major contributor to mortality and morbidity. One to two percent of individuals worldwide currently suffer from AF[1] and its prevalence is expected to increase 2.5-fold in the next 40 years.[2] Over the past decade, catheter ablation has emerged as a potential approach to treat AF. However, in the subset of patients with persistent AF (PsAF), who have extensive atrial fibrotic remodelling,[3–5] the success rate of catheter ablation is extremely low (~50%)[6] and the process involves procedures that are tedious and time-consuming. Moreover, even in AF patients in whom ablation procedures are initially successful, post-procedure arrhythmias are common, with left atrial flutter (LAFL) occurring in up to 31% of cases.[7,8] The re-entrant circuit in these cases is often located in fibrotic tissue of the LA,[9] requiring subsequent ablation procedures that are technically challenging and non-systematic.[10–12]

As such, there is an urgent need to develop new approaches for the treatment of complex atrial arrhythmias that incorporate understanding of contributions from the fibrotic remodelled tissue and are tailored to the individual patient. Given that late gadolinium-enhanced magnetic resonance imaging (LGE-MRI) can now be used to reconstruct each patient's unique fibrotic substrate,[13–15] the ultimate hope is that information extracted from such scans can be leveraged to guide powerful new ablation approaches that are custom-tailored to render the initiation and perpetuation of atrial re-entry in the given patient impossible. However, attempts to put this into practice have been greatly hindered by a dearth of understanding regarding how each individual's specific distribution of fibrotic tissue affects arrhythmia dynamics. This review summarizes findings from a major recent research thrust that seeks to address this knowledge gap by using patient-derived LGE-MRI-based computational models of the fibrotic atria to develop novel mechanistic insights and ablation strategies relevant to personalized treatment of atrial arrhythmias.

Modelling the fibrotic substrate for atrial arrhythmias

In an attempt to elucidate the mechanisms in the fibrotic substrate leading to altered conduction and those responsible for the re-entrant drivers and organization of atrial arrhythmias, early models of the fibrotic atria accounted for different aspects of fibrotic remodelling in a variety of ways. The simplest model representation of atrial struc-

* Corresponding author. Tel: 410 516 4375; fax: 410 516 5294. *E-mail address*: ntrayanova@jhu.edu

tural remodelling was based on the assumption that gap junction remodelling (C×43 down-regulation, hypophosphorylation, and lateralization of connexin-43 [C×43]) occurs throughout the atria in a uniform fashion. Two such studies were conducted: one assumed that the coupling strength between computational cells was decreased (Cx43 down-regulation, hypophosphorylation only),[16] while the other modelled increased anisotropy throughout the LA (representing both aspects of Cx43 remodelling).[17] The first simulation study[16] showed that decreasing the coupling between cells slowed conduction and decreased the wavelength, further perpetuating AF. The second study[17] demonstrated that increased anisotropy throughout the fibrotic human LA was an additional mechanism for the breakup of ectopic waves emanating from the pulmonary veins (PVs) into multiple re-entrant circuits; higher anisotropy ratios resulted in sustained re-entrant activity even though the ectopic focus was no longer present. Similar conclusions were obtained from a human atrial model[18] where the locations of the fibrotic (i.e., high-anisotropy-ratio) regions were implemented from patient MRI-LGE scans.

The next component of fibrosis, collagen deposition, was first represented in seminal studies by Spach *et al.*[19] who simulated diffuse fibrosis by removing lateral gap junctions from a model of human atrial tissue. Increased heterogeneity in intercellular coupling was found to lead to vulnerability for partial wave block and re-entry. Subsequently, collagen deposition has been represented in models as insulating barriers in several ways. In the first example,[20] this was achieved by randomly removing electrical connections between two 2D layers of atrial tissue (endocardial and epicardial) to model increased dissociation between these two layers (a form of reactive interstitial fibrosis), mimicking experimental observations in goats;[21] this resulted in a number of AF re-entrant waves that was significantly higher than that in the case without dissociation, exacerbating AF complexity. These findings were later complemented by experiments involving simultaneous epicardial and endocardial optical mapping in sheep atria,[22] which showed that AF substrate complexity is exacerbated by transmural discordance due to uncoupling of layers. Subsequent studies introduced a set of random collagenous septa disconnecting cardiac fibres in the transverse direction[23] (i.e., reactive interstitial fibrosis again) or incorporated non-conductive regions of various sizes throughout the tissue[24–27] (i.e., reparative fibrosis), either randomly throughout the atria, or based on imaging data. The increase in collagen content in the interstitial spaces between fibres was not found to affect longitudinal conduction,[25] but caused slowed propagation in transverse direction, with the degree of slowing dependent of the length of the collagenous septa.[23] Most recently, Vigmond *et al.*[28] showed that simulation of conduction obstacles derived from LGE-MR images of AF patient atria gave rise to excitation patterns resembling near-threshold percolation (i.e., slow and tortuous fluid flow through a porous medium) (*Figure 1A and B*). Wavefronts propagating in these models produced electrocardiographic measurements consistent with measurements obtained during mapping of AF in patients (i.e., amplitude and fractionation of electrograms in fibrotic regions; *Figure 1C–E*). Critically, the authors also demonstrated that this percolation-like excitation dynamic gave rise to arrhythmogenesis, with biphasic dependence between the density of fibrotic obstacles and the likelihood of initiating re-entry (*Figure 1F*).

Atrial models incorporating transverse collagen deposition[24–26] (as in reparative fibrosis) have highlighted the significant interruption and disarray in atrial conduction patterns caused by it. Importantly, collagen deposition rather than C×43 remodelling was found to be the major factor in atrial conduction disturbances under heart failure conditions.[25] Furthermore, it was established that not only the total amount, but also the specific spatial distribution of collagen deposition (e.g., as generated by a stochastic algorithm) governed the occurrences of conduction block.[26] To evaluate the consequences of structural remodelling on AF dynamics in the posterior left atrium (LA), Tanaka *et al.*[24] used 2D models of transmural posterior LA sections generated from histological data; patchy distributions of collagen were also reconstructed from those data. Simulations demonstrated that whether the mechanism sustaining AF was re-entrant or focal, fibrous patches of large size were the major factor responsible for the different dynamics of AF waves in remodelled vs. control hearts; they anchored re-entrant circuits and impaired wave propagation to generate delays and signal fractionation.

Computational modelling has also been used to improve understanding of complex inherited arrhythmia-causing diseases in which a genetic mutation causes changes in both cellular electrophysiology and structural remodelling. Wolf *et al.*[29] explored mechanisms of AF perpetuation in individuals with Ankyrin-B dysfunction by conducting simulations in 2D models of atrial tissue incorporating consequences of the disease at both the cell scale (abbreviated action potential duration [APD] due to defective membrane targeting of I_{CaL}) and the tissue scale (conduction slowing due to increased fibroblast proliferation and collagen deposition). In models including either diffuse or clustered regions of fibrotic remodelling, the authors observed shorter functional lines of conduction block and a complex relationship between the duration of induced re-entry and the size of the simulated tissue, with a high incidence of re-entry-terminating conduction block in both small ($\leq$7 cm^2) and large ($\geq$12 cm^2) rectangular domains; the spatial pattern of fibrosis (i.e., diffuse vs. clustered) did not affect these results. When the same simulations were repeated with cell-level effects of Ankyrin-B only (i.e., in the absence of fibrosis), this behaviour was eliminated, suggesting that tissue-scale fibrotic remodelling may be the primary underlying source of complex arrhythmia dynamics in patients with the corresponding inherited disease. Importantly, the authors also presented results suggesting a similar multi-scale mechanism explains aberrant sinoatrial node behaviour in the same cohort.

A third component of fibrotic remodelling, fibroblast proliferation, and phenotype switching has also been represented in computational models of the atria. This is particularly relevant in view of the fact that fibroblasts, in addition to being part of the structural remodelling of the atria, could potentially also exert electrophysiological influences on neighbouring myocytes, either through electrical coupling[30] or via paracrine effects.[31] The first study to explicitly incorporate fibroblast presence as a representation of fibrotic remodelling was the 2D atrial model by Ashihara *et al.*[32] Within the fibrotic region, coupling of fibroblasts (kinetics governed by a fibroblast ionic model) to atrial myocytes caused shorter APD, slower conduction, and lower excitability as well as spiral wave breakups. This effect was exacerbated when fibroblast density increased. Interestingly, when fibroblasts were substituted by collagen in the model, wave breakups were not observed. It needs to be noted, however, that the role of

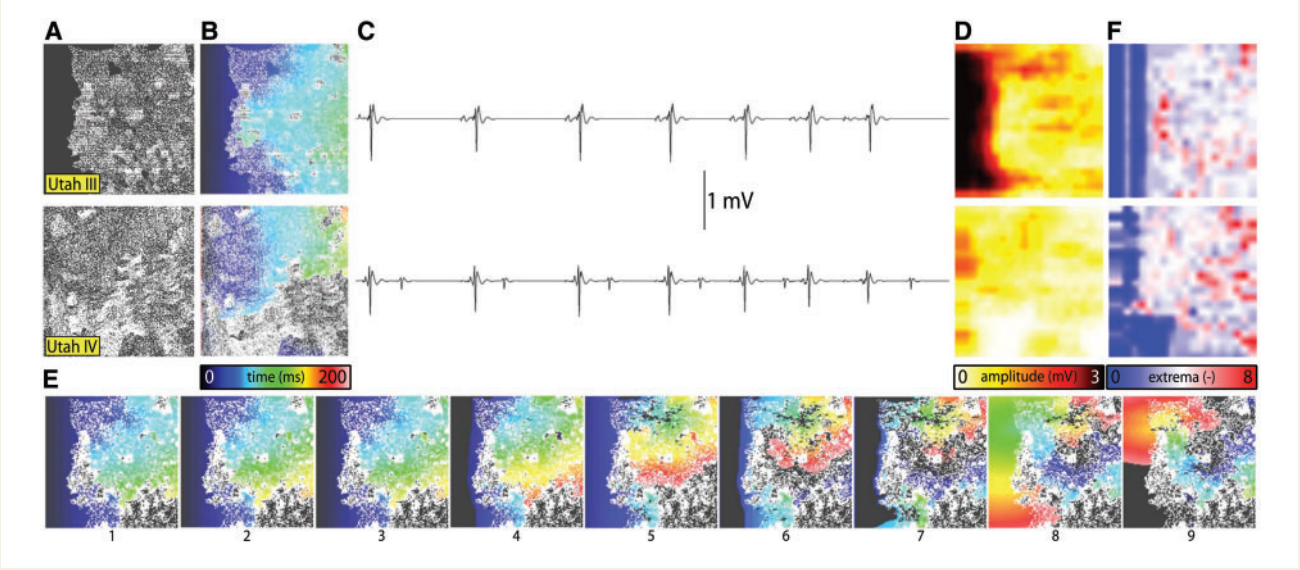

Figure 1 Wavefront propagation in 2D atrial tissue models with fibrosis patterns derived from AF patient LGE-MRI. (*A–E*) For models derived from scans of Utah III (top) and Utah IV (bottom) patients: fibrosis patterns, with brighter voxel intensity indicating higher LGE (*A*); activation times in response to pacing at left edge of model (*B*); bipolar electrogram signals recorded from a location 1 mm above the centre of each model (*C*), along with accompanied by maps of electrogram amplitude (D) and extrema count (*E*). (*F*) Panels 1–7 show activation times in a model based on scans from a Utah III patient in response to seven consecutive stimuli (same pacing electrode and colour scale as (*B*)). Panels 8–9 illustrate initiation of reentry due to propagation near the percolation threshold within the fibrotic tissue region. With permission from Vigmond *et al.*[28]

myofibroblasts in altering action potential dynamics via gap-junction coupling remains controversial.

Finally, a new research thrust has focused on the investigation of differences in prevalence of perimysial fibrosis (i.e., clefts between bundles of myocytes) and endomysial fibrosis (i.e., clefts between myocytes *within* bundles) between different stages of progressive AF. Using an experimental goat model, Verheule *et al.*[33] showed that endomysial remodelling was more severe in animals with long-term AF (LT, 6 months) than in those with short-term AF (ST, 3 weeks); these two animal models are roughly analogous to permanent and persistent AF in humans, respectively. Interestingly, no significant difference in perimysial fibrosis was observed between LT and ST groups. Excess sub-epicardial endomysial fibrosis had prominent effects on atrial electrophysiology in LT goats, including significantly reduced wave size and increased anisotropy. When the authors incorporated these features in a computational model with 2D epicardial and endocardial layers coupled by discrete transmural bundles, they observed that the LT variant had more distinct waves and more epicardial breakthroughs in each AF cycle. The resulting loss of synchronization was consistent with experimental observations, providing a plausible explanation for differences in arrhythmia characteristics between persistent and permanent AF patients.

The advances in understanding of the fibrotic substrate described in the section above are all important building blocks in the construction of patient-derived organ-scale atrial models, which are the focus of the remainder of this review. For a detailed comparison of the different methodologies employed to model the fibrotic substrate, the reader is referred to the article by Roney *et al.*[34] in this supplement.

Image-based 3D modelling of the fibrotic left atrium

The first three major elements of fibrotic remodelling discussed in the preceding (gap-junction remodelling, collagen deposition, and myofibroblast proliferation), were combined together by McDowell *et al.*[35,36] in an 3D LA model reconstructed from MRI-LGE scans of a patient with permanent AF. This model was the first to accurately capture not only the 3D patient-specific atrial geometry, but also each individual's distribution of fibrotic lesions in the atria. Electrophysiological remodelling associated with persistent AF was also incorporated.[37,38] The model was used to examine the mechanisms for AF initiation by PV ectopic stimulation. The study found that for fibrotic lesions typical of human remodelled atria under the conditions of persistent AF, gap junction remodelling in the fibrotic lesions was a necessary but not sufficient condition for the development of AF following a PV ectopic beat. The sufficient condition was myofibroblast proliferation in these lesions, where myofibroblasts exerted either electrotonic or paracrine influences on myocytes within the lesions. Deposition of collagen in the lesions exacerbated the myofibroblasts' paracrine or electrotonic effects by additionally shortening regional APD.

In a subsequent study that used the same methodology, McDowell *et al.*[39] provided the first proof-of-concept that patient-specific models combining atrial structure, fibrosis distribution from clinical MRI, and representation of remodelled atrial electrophysiology could be used to predict the optimal ablation targets in patients. The study reconstructed four patient-specific atrial models, each of different

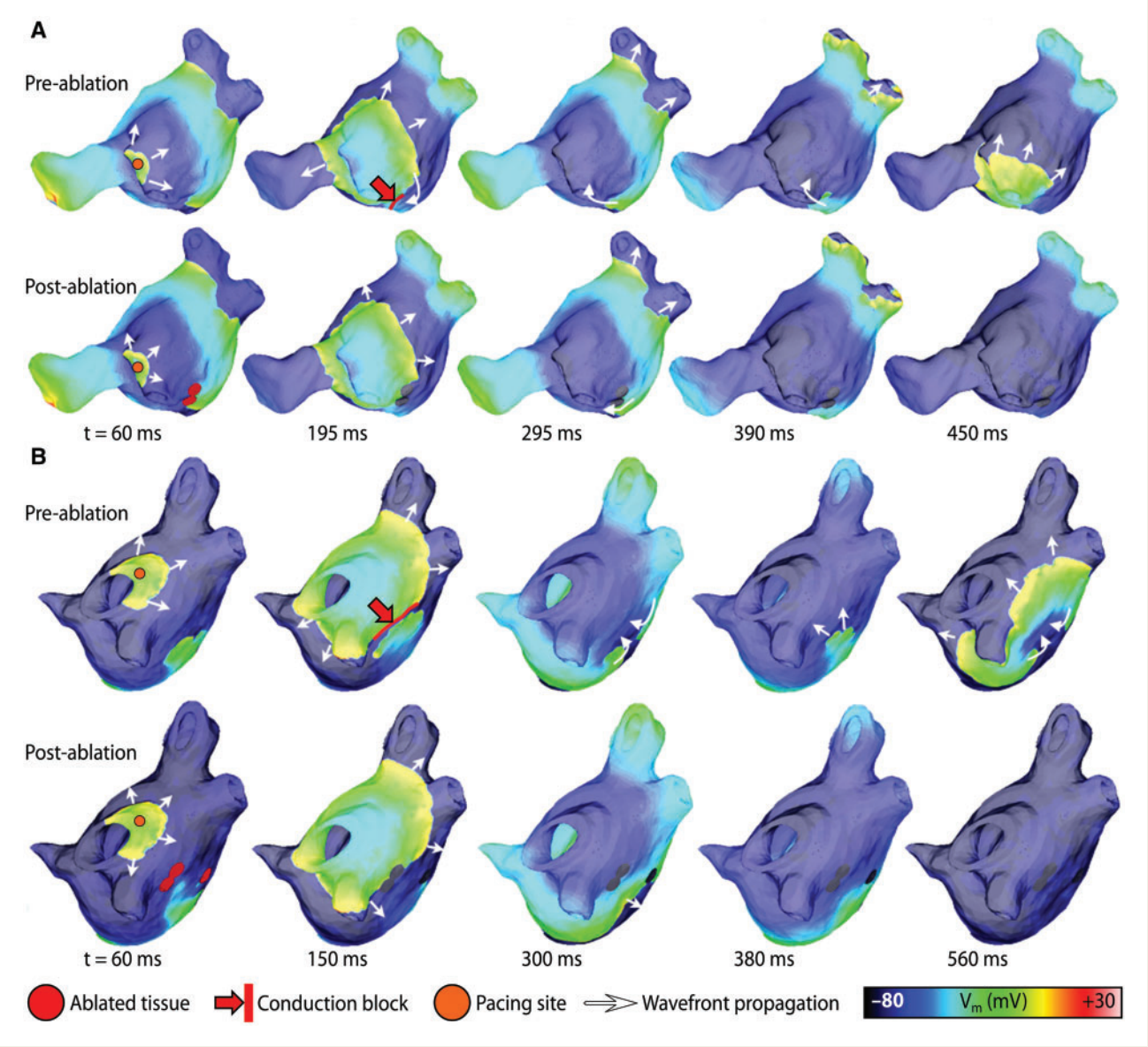

Figure 2 Effect of ablating tissue enclosing organizing centres of reentry in patient-specific left atrial models. (*A*) For a Utah III patient, sequential maps of transmembrane voltage (V_m) illustrate the response to ectopic pacing from the left pulmonary veins, before (top) and after (bottom) the simulation of ablation lesions, as described in the text. (*B*) Same as (*A*) but for a Utah IV patient. With permission from McDowell *et al.*[39]

Utah fibrosis score,[40] in which two had persistent AF associated with fibrosis, and analysed arrhythmia dynamics to determine the targets of ablation. When the restricted regions encompassing the meander of the persistent phase singularities were modelled as ablation lesions, AF could no longer be induced (*Figure 2*). The results from this study suggested that a patient-specific modelling approach to identify non-invasively AF ablation targets prior to the clinical procedure is feasible.

While the studies discussed in this section established the basic elements for image-based modelling of electrophysiology in the fibrotic atria and yielded important mechanistic insights regarding the initiation, perpetuation, and termination of AF, they focused exclusively on simulations of the LA. Given the fact that AF-perpetuating re-entrant sources have also been found to localize in the right atrium[41] and have even been directly targeted for catheter ablation,[42] a major priority for the next generation of patient-specific simulations (as discussed in the following sections) was the development of models representing both the right and left atria.

Fibrotic determinants of re-entrant driver localization

The first computational assessment of the relationship between fibrosis and re-entrant driver dynamics was conducted in a 3D anatomical model of the human atria originally derived by Harrild and

Henriquez from CAD drawings.[43] Krogh-Madsen *et al.*[16] examined the behaviour of AF-perpetuating re-entrant sources in the presence of structural fibrotic remodelling with or without cell-scale electrophysiology remodelling. The effect of fibrosis was represented by uniformly decreasing conductivity throughout the atria by up to 50%, resulting in a ~40% increase in the time required for full atrial activation in response to sinus pacing; cell-scale remodelling was represented by modifying key ionic currents as in previous studies,[37] resulting in a ~20% decrease in APD. As discussed in the previous section, both types of remodelling decreased cardiac wavelength, which is the product of APD and conduction velocity. When re-entry was initiated via a cross-shock protocol, the authors found that both arrhythmia duration and the maximal number of simultaneously occurring filaments (i.e., number of concomitant re-entrant drivers) was shown to be inversely proportional to wavelength. Interestingly, in simulations conducted with either cellular remodelling only or fibrotic remodelling only, the authors exclusively observed arrhythmia perpetuated by macroscopic anatomical re-entry (e.g., wavefront propagation around the pulmonary veins, inferior/superior vena cava, or tricuspid annulus), which is more characteristic of atrial flutter than AF. In contrast, when both types of remodelling were included, numerous episodes of arrhythmia driven by 'un-anchored' re-entrant drivers in the left or right atrial walls were observed. Thus, this study produced the crucial insight that computer models must incorporate changes due to both cell-scale electrophysiological remodelling and fibrotic in order to facilitate the simulated induction of AF-like arrhythmias. However, the important question of the exact relationship between the spatial pattern of fibrotic tissue and AF re-entrant dynamics remained unanswered.

More recently, studies[44,45] on fibrosis and AF have focused on addressing that gap in the literature by using 3D bi-atrial patient-specific models incorporating the individual's unique fibrotic distribution. A question of particular importance is how the specific fibrotic distribution in each heart impacts the locations of AF-perpetuating re-entrant drivers. These studies used a large number of patient-specific atrial models ($n = 20$) with individualized fibrosis distribution reconstructed from LGE-MRI. In addition to including action potential changes associated with persistent AF, fibrotic regions were represented with remodelled electrophysiology, anisotropy, and conduction properties, but without representing explicitly any electrophysiological effects associated with the controversial myocyte-fibroblast coupling. Instead, ionic current modifications were implemented consistent with electrophysiological changes that atrial myocytes undergo when subjected to elevated levels of transforming growth factor β1 (TGF-β1), a key component of the fibrogenic signalling pathway.[46,47] Conductivity values and anisotropy ratios in fibrotic regions reflected decreased intercellular coupling due to replacement fibrosis, collagen deposition (interstitial fibrosis), and gap junction remodelling.[25,48] In this manner, the representation of fibrotic remodelling not only better reflected new experimental data, but also ensured computational tractability of studies involving a large number of patient-specific atrial models.

In all 20 patient specific models, programmed electrical stimulation was simulated to determine the AF propensity of the fibrotic substrate. Arrhythmias perpetuated by re-entrant drivers were induced in 13/20 models. *Figure* 3A shows an example of re-entrant arrhythmia induced in one such model, with inset panels highlighting the re-entrant driver. Qualitatively, it was observed that phase singularities associated with the re-entrant driver persisted near fibrosis cluster boundaries (*Figure 3B*). In each model, characteristics of the fibrosis spatial pattern were analysed by computing local spatial metrics for a surrounding volume within 1.5 mm spherical kernel around each point (*Figure 3C*). Metrics included fibrosis density (FD; proportion of LGE tissue) and Shannon entropy (FE; i.e. degree of local disorganization). This analysis revealed a fibrosis spatial pattern that consistently harboured all re-entrant driver-associated phase singularities in all 13 patient-specific models: these regions had high FD and FE values ($\geq$0.45, orange coloured regions) compared to tissue in the rest of the atria (*Figure 3D*). This characteristic pattern corresponded to a subset of boundaries between fibrotic and non-fibrotic myocardium in which there was extensive intermingling of the two tissue types. Notably, phase singularities were never observed in regions of dense fibrotic tissue (i.e. sites with high FD and low FE, as indicated in *Figure 3C*).

To further understand the relationship between fibrosis spatial pattern and re-entrant driver localization, 2D histograms were constructed to compare the combined FD and FE values corresponding to regions where the fibrosis pattern favoured the formation of re-entrant drivers (i.e., pro-re-entrant driver tissue, *Figure 4A*) and elsewhere in the atria (*Figure 4B*). This established the characteristic parameter ranges of pro-re-entrant driver regions as $FD = 0.63 \pm 0.17$ and $FE = 0.51 \pm 0.14$, which were distinct from values elsewhere in the atria ($FD = 0.13 \pm 0.19$, $FE = 0.18 \pm 0.22$). Based on this observation, a supervised machine learning algorithm was used to derive a highly sensitive and specific polynomial equation for discriminating between regions favourable and non-favourable for re-entrant driver localization based on FD and FE values. Tissue regions identified as pro-re-entrant driver by machine learning corresponded to a subset of fibrotic region boundary zones (*Figure 4C*). Although the proportion of all atrial tissue in all models that had this characteristic pattern was relatively small ($13.79 \pm 4.93\%$), the subregion was found to contain an impressive majority ($83.50 \pm 2.35\%$) of all re-entrant driver-associated phases singularity sites. Excitingly, when trajectories of re-entrant driver organizing centres observed *in vivo* via electrocardiographic imaging (ECGI) were mapped into the corresponding patient models, a large proportion ($56.7 \pm 9.1\%$) were found to be located in the compact tissue area (i.e., $13.79 \pm 4.93\%$ of the overall atrial volume) that was classified a pro-re-entrant driver by the above-described method (*Figure 4D*). Overall, this study demonstrated that in personalized models of AF under the conditions of fibrosis, the phase singularities of the persistent re-entrant circuits were exclusively harboured in regions with a complex but quantitatively well-defined fibrosis spatial pattern. The study concluded that identifying locations with such properties could help optimize AF ablation.

Based on the findings described above, a follow-up simulation study[45] examined whether the prevalence of regions with an intermingling of fibrotic and non-fibrotic tissue correlates with the inducibility of AF. If so, could this metric serve as a better predictor of AF inducibility than total atrial fibrosis burden? The latter quantity (total fibrosis burden; FB) has been previously linked to higher risk of persistent AF.[49] Using the same set of patient-specific models described above, the prevalence of regions with highly intermingled fibrotic and non-fibrotic tissue in each case was assessed by median and upper

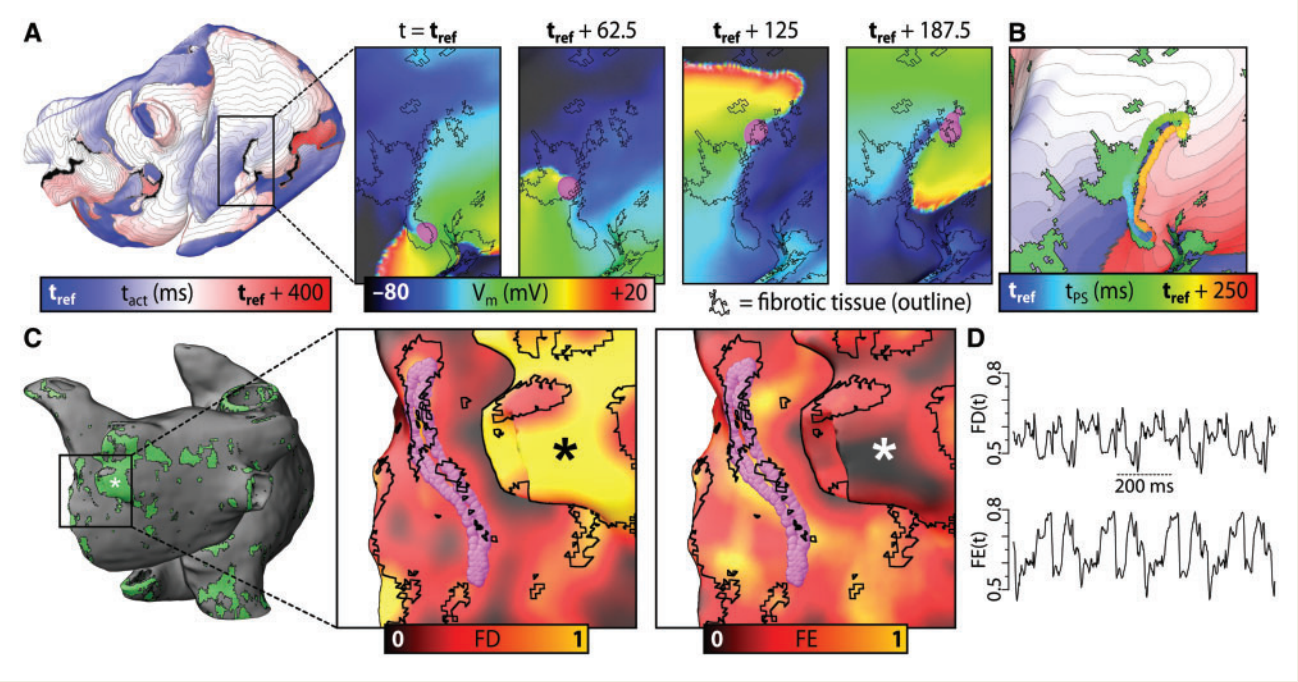

Figure 3 Relationship between reentrant driver localization and fibrosis spatial pattern in patient-specific models of persistent AF. (*A*) Map showing activation times with respect to reference time (t_{ref}) for a reentrant driver near the inferior vena cava. Inset panels: maps of transmembrane voltage (V_m). Reentrant driver-associated phase singularities are marked by magenta spheres. (*B*) Phase singularity trajectory over time superimposed on activation map with fibrosis spatial pattern (green). (*C*) Distribution of fibrotic tissue (green) for a different patient-specific atrial model than in panels (*A*) and (*B*). Inset panels: maps of FD and FE metrics (see text) used to quantitatively characterize fibrosis spatial pattern, with fibrotic tissue boundaries and phase singularity trajectories shown as in (*A*). Asterisk: region with high FD, low FE. (*D*) Time series plots of FD and FE at phase singularity locations for the case shown in (*C*); values range from 0.45–0.8. With permission from Zahid *et al.*[44]

quartile values of each unique FD metric distribution (FD_{50} and FD_{75}, respectively). Simulations demonstrated that atrial models in which rapid pacing did not induce AF had low both FB ($\leq$ 11%) and FD_{75} ($\leq$ 0.1) values. In AF-inducible models, higher inducibility was associated with increased FB and D_{75}. Inducibility was correlated both with FB and with FD_m, a linear combination of FD_{50} and FD_{75}. Statistical analysis demonstrated that FD_m had a higher predictive power than FB. This simulation study demonstrated that fibrosis spatial pattern analysis could be a novel avenue for persistent AF risk stratification. This is particularly noteworthy in light of recent clinical findings that showed a lack of association between the regional or global extent of LGE areas and AF-perpetuating re-entrant drivers,[50] suggesting that more robust quantitative metrics (such as FD_m or local maps of FD and FE, as discussed above[44]) could provide a better indication of the spatial localization of re-entrant drivers in the fibrotic atria.

Model-based prediction of optimal ablation strategies

Among the many ultimate goals of patient-specific cardiac arrhythmia modelling, one of the most ambitious is the development of simulation-based personalized treatment plans for optimal ablation procedures. Recently, a major step towards this object was taken with the publication of a study[51] that compared model-predicted optimal ablations with clinical lesions that rendered arrhythmia non-inducible. Specifically, this study was carried out in a cohort of patients who were successfully treated for AF via catheter ablation but experienced recurrent post-procedure left atrial flutter (LAFL). Ten patient-specific atrial models were reconstructed from LGE-MRI using the same approach described in the previous section. Left atrial flutter was induced in 7/10 models and re-entrant cycle lengths were consistent with clinically observed values in the corresponding patients. In each case, re-entrant wave propagation was then abstracted as an electric flow network, which facilitated the application of principles from graph theory, including the identification of a so-called 'minimum cut' (MC)—i.e., the point in the network whose blockage separated the flow into two discontinuous components.[52] For 4/7 cases, ablation of MC locations rendered LAFL completely non-inducible (*Figure 5*, left panels); for the other three cases, rapid pacing of post-ablation models induced arrhythmias that were slower and associated with different re-entrant circuits than the ablated LAFL morphologies. When a second iteration of the MC ablation approach was applied to these patient models, they were rendered completely non-inducible.

Importantly, the resulting MC-based targets, which in each case encompass the minimum volume of ablated tissue necessary to abolish LAFL inducibility in silico, were similar location but smaller than clinical ablation lesions that successfully terminated LAFL in the corresponding patients (2.8 $\pm$ 1.5 cm vs. 4.8 $\pm$ 1.7 cm, $P < 0.05$). As such,

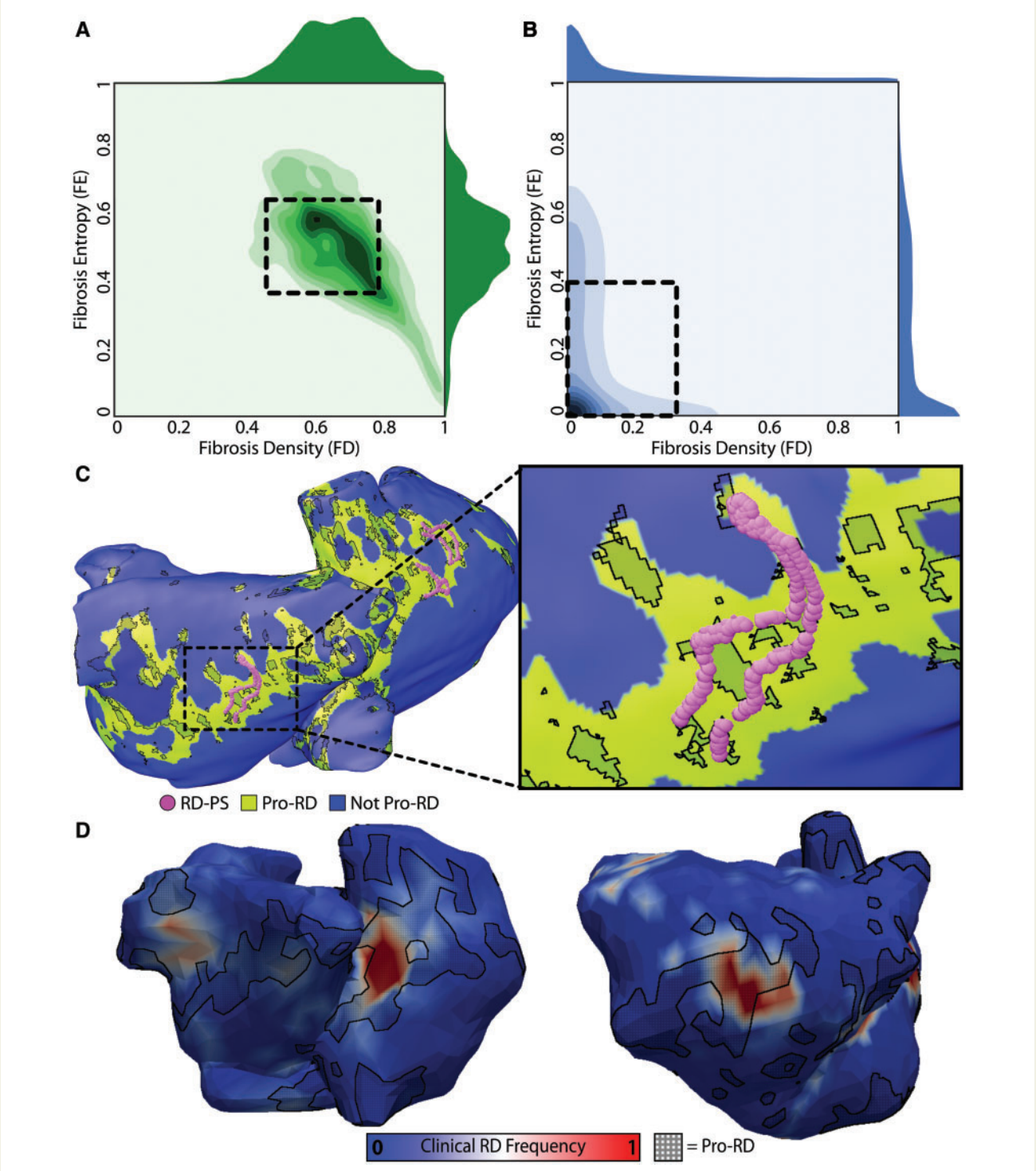

Figure 4 Quantitative characteristics of fibrosis spatial pattern in atrial regions that harbour reentrant drivers of persistent AF. (*A*) 2D histogram showing the values of fibrosis density and entropy (FD and FE) metrics at locations of phase singularities associated with reentrant drivers induced by rapid pacing in 13 patient-specific models. 1D histograms of FD (above) and FE (right) values are also shown. Boxed region: values within one standard deviation of mean FD and FE values ($0.37 \leq FE \leq 0.65$; $0.46 \leq FD \leq 0.80$). (*B*) Same as (*A*) but for locations where phase singularities were never observed. Boxed region: $0 \leq FE \leq 0.40$; $0 \leq FD \leq 0.32$. (*C*) Locations of all reentrant driver-associated phase singularities for a particular patient-derived atrial model overlaid on map showing distribution of tissue regions with the fibrosis spatial pattern identified by machine learning (see text) as favourable to the initiation and perpetuation of reentrant arrhythmia (green). (*D*) Maps of reentrant driver-associated phase singularity frequency obtained via ECGI during persistent AF episodes in two patients. Regions classified as favourable to reentrant driver localization by machine learning (i.e., same as green regions in (*C*)) are overlaid with a black crosshatched pattern. With permission from Zahid *et al.*[44]

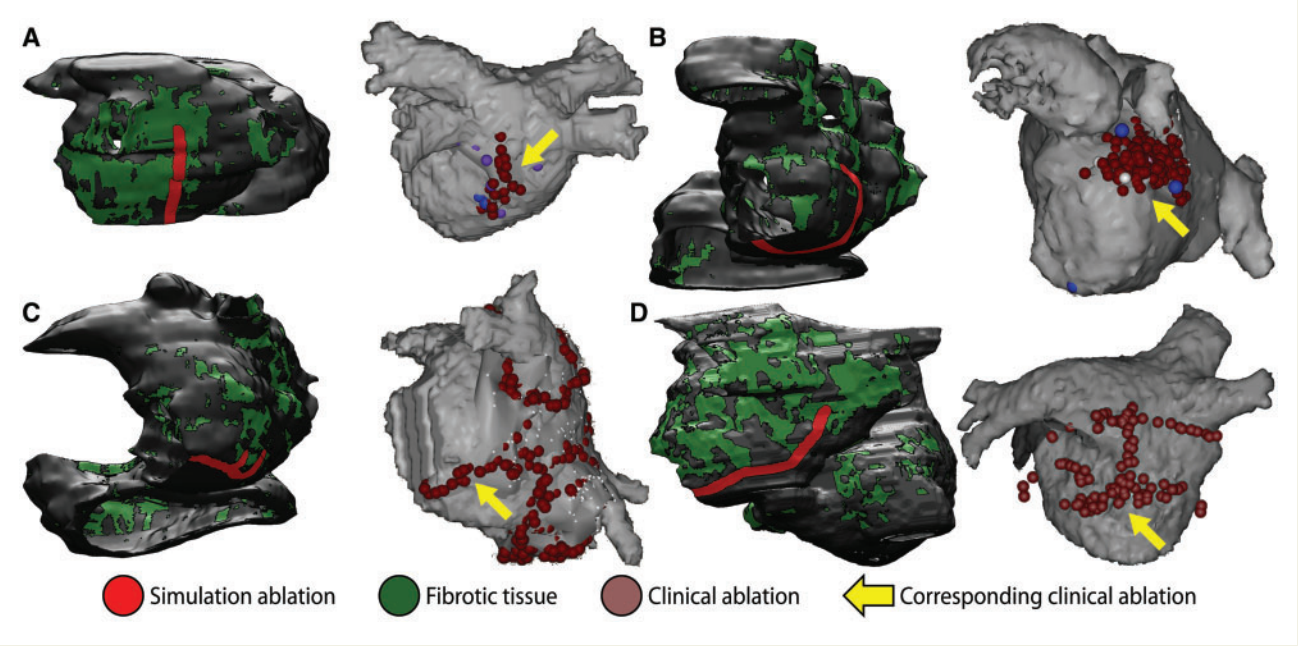

Figure 5 Simulations in patient-specific atrial models reconstructed from LGE-MRI can be used to predict optimal ablation targets for LAFL. (*A–D*) For four patients in the LAFL cohort, "minimum cut" ablations in the atrial model (left) are compared to lesions that were applied during successful clinical ablation procedures (right). Matching lesions are indicated with yellow arrows. With permission from Zahid *et al.*[51]

this study provided important proof of concept for the use of simulations conducted pre-procedure in patient-specific models derived from clinical LGE-MRI scans to successfully plan clinical ablation procedures.

Another recent study by Bayer *et al.*[53] used a bi-layer computational model of the LA incorporating fibrotic remodelling using a probabilistic approach based on LGE-MRI data from PsAF patients (the same methodology described by Vigmond *et al.*[28]) to explore the relative efficacy of three different strategies for radio-frequency ablation. The first approach tested was pulmonary vein isolation (PVI) with additional lesions along the LA roof and connecting to the mitral annulus; this was found to be ineffective except in cases where re-entrant drivers happened to be initiated in locations near the PVs. The second strategy was the execution of ablation lesions of different shapes (circles, perforated circles, lines, crosses) and sizes (0.5–1.5 cm) at sites where density of AF-perpetuating organizing centres (i.e., phase singularities—PSs) was high. In contrast to PVI plus lines, this approach proved highly effective, especially when the largest (1.5 cm) perforated circle-shaped lesions were used (positive correlation between successful lesion locations and PS density: $r > 0.75$, $P < 0.05$). Finally, the authors tested the efficacy of a novel approach based on executing ablation lines that streamlined the left atrial activation sequence observed during sinus rhythm. For $n = 5$–8 evenly spaced lines, this strategy was very effective, resulting in immediate AF termination in all cases. Although these results are compelling, suggesting the theoretical existence of a 'one size fits all' approach for persistent AF ablation, the authors correctly note that the translation of the streamlining ablation approach to clinical application would be a tremendous technical challenge.

Concluding remarks

As this review demonstrates, recent studies have leveraged personalized computer models of the atria to elucidate the mechanisms of arrhythmia initiation, perpetuation, and termination in the fibrotic substrate. Notably, this research thrust has been paralleled by similar efforts to develop and utilize patient-specific models of ventricular arrhythmias that involve structural and fibrotic remodelling.[54,55] This includes studies aiming to estimate ablation targets for scar-related ventricular tachycardia[56] and stratify risk of lethal arrhythmias in post-myocardial infarction patients, including individuals for whom insertion of implantable defibrillators is clinically indicated[57] and (as discussed elsewhere in this supplement) those for whom it is not.[58]

Furthermore, the field has now progressed to an exciting stage where computer modellers and clinicians are on the precipice of a truly thrilling collaboration that will involve the execution of catheter ablations in patients based on optimal treatment plans derived from pre-procedure simulations that take into account each individual's unique pattern of fibrotic structural remodelling. As this fascinating research trajectory continues to be explored in the future, the usefulness of its findings will depend on continuous adaptation and integration of new elements, including model redesign and evaluation, improvements in the execution time of biophysically detailed atrial models, implementation of consistent strategies for comparison with experimental and clinical measurements, and investment in efforts to ensure repeatability and consistency of simulation results.

Funding

This work was supported by American Heart Association 16-SDG-30440006 (to P.M.B.); by an NSF Graduate Research Fellowship and an ARCS Foundation Award (to S.Z.); and by the Johns Hopkins Medicine Discovery Fund, NIH DP1-HL123271, and NSF CDI 1124804 (to N.A.T.).

Conflict of interest: none declared.

References

1. Andrade J, Khairy P, Dobrev D, Nattel S. The clinical profile and pathophysiology of atrial fibrillation: relationships among clinical features, epidemiology, and mechanisms. *Circ Res* 2014;**114**:1453–68.
2. Go AS, Hylek EM, Phillips KA, Chang Y, Henault LE, Selby JV *et al*. Prevalence of diagnosed atrial fibrillation in adults: national implications for rhythm management and stroke prevention: the AnTicoagulation and Risk Factors in Atrial Fibrillation (ATRIA) study. *JAMA* 2001;**285**:2370–5.
3. Oakes RS, Badger TJ, Kholmovski EG, Akoum N, Burgon NS, Fish EN *et al*. Detection and quantification of left atrial structural remodeling with delayed-enhancement magnetic resonance imaging in patients with atrial fibrillation. *Circulation* 2009;**119**:1758–67.
4. Marrouche NF, Wilber D, Hindricks G, Jais P, Akoum N, Marchlinski F *et al*. Association of atrial tissue fibrosis identified by delayed enhancement MRI and atrial fibrillation catheter ablation: the DECAAF study. *JAMA* 2014;**311**:498–506.
5. Cochet H, Mouries A, Nivet H, Sacher F, Derval N, Denis A *et al*. Age, atrial fibrillation, and structural heart disease are the main determinants of left atrial fibrosis detected by delayed-enhanced magnetic resonance imaging in a general cardiology population. *J Cardiovasc Electrophysiol* 2015;**26**:484–92.
6. Verma A, Jiang CY, Betts TR, Chen J, Deisenhofer I, Mantovan R *et al*. Approaches to catheter ablation for persistent atrial fibrillation. *N Engl J Med* 2015;**372**:1812–22.
7. Gerstenfeld EP, Callans DJ, Dixit S, Russo AM, Nayak H, Lin D *et al*. Mechanisms of organized left atrial tachycardias occurring after pulmonary vein isolation. *Circulation* 2004;**110**:1351–7.
8. Daoud EG, Weiss R, Augostini R, Hummel JD, Kalbfleisch SJ, Van Deren JM *et al*. Proarrhythmia of circumferential left atrial lesions for management of atrial fibrillation. *J Cardiovasc Electrophysiol* 2006;**17**:157–65.
9. Miyazaki S, Shah AJ, Kobori A, Kuwahara T, Takahashi A. How to approach reentrant atrial tachycardia after atrial fibrillation ablation. *Circ Arrhythm Electrophysiol* 2012;**5**:e1–7.
10. Stevenson WG, Sager PT, Friedman PL. Entrainment techniques for mapping atrial and ventricular tachycardias. *J Cardiovasc Electrophysiol* 1995;**6**:201–16.
11. Patel AM, d'Avila A, Neuzil P, Kim SJ, Mela T, Singh JP *et al*. Atrial tachycardia after ablation of persistent atrial fibrillation: identification of the critical isthmus with a combination of multielectrode activation mapping and targeted entrainment mapping. *Circ Arrhythm Electrophysiol* 2008;**1**:14–22.
12. Jais P, Shah DC, Haissaguerre M, Hocini M, Peng JT, Takahashi A *et al*. Mapping and ablation of left atrial flutters. *Circulation* 2000;**101**:2928–34.
13. McGann C, Akoum N, Patel A, Kholmovski E, Revelo P, Damal K *et al*. Atrial fibrillation ablation outcome is predicted by left atrial remodeling on MRI. *Circ Arrhythm Electrophysiol* 2014;**7**:23–30.
14. Khurram IM, Beinart R, Zipunnikov V, Dewire J, Yarmohammadi H, Sasaki T *et al*. Magnetic resonance image intensity ratio, a normalized measure to enable interpatient comparability of left atrial fibrosis. *Heart Rhythm* 2014;**11**:85–92.
15. Parmar BR, Jarrett TR, Burgon NS, Kholmovski EG, Akoum NW, Hu N *et al*. Comparison of left atrial area marked ablated in electroanatomical maps with scar in MRI. *J Cardiovasc Electrophysiol* 2014;**25**:457–63.
16. Krogh-Madsen T, Abbott GW, Christini DJ. Effects of electrical and structural remodeling on atrial fibrillation maintenance: a simulation study. *PLoS Comput Biol* 2012;**8**:1002390.
17. Plank G, Prassl AJ, Wang JI, Seeman G, Scherr D, Sanchez-Quintana D *et al*. Atrial fibrosis promotes the transition of pulmonary vein ectopy into reentrant arrhythmias *Heart Rhythm*. 2008:**5**:S78.
18. Krueger MW, Rhode KS, O'Neill MD, Rinaldi CA, Gill J, Razavi R *et al*. Patient-specific modeling of atrial fibrosis increases the accuracy of sinus rhythm simulations and may explain maintenance of atrial fibrillation. *J Electrocardiol* 2014;**47**:324–8.
19. Spach MS, Heidlage JF, Dolber PC, Barr RC. Electrophysiological effects of remodeling cardiac gap junctions and cell size: experimental and model studies of normal cardiac growth. *Circ Res* 2000;**86**:302–11.
20. Gharaviri A, Verheule S, Eckstein J, Potse M, Kuijpers NH, Schotten U. A computer model of endo-epicardial electrical dissociation and transmural conduction during atrial fibrillation. *Europace* 2012;**14**(Suppl 5):v10–v16.
21. Eckstein J, Maesen B, Linz D, Zeemering S, van Hunnik A, Verheule S *et al*. Time course and mechanisms of endo-epicardial electrical dissociation during atrial fibrillation in the goat. *Cardiovasc Res* 2011;**89**:816–24.
22. Gutbrod SR, Walton R, Gilbert S, Meillet V, Jais P, Hocini M *et al*. Quantification of the transmural dynamics of atrial fibrillation by simultaneous endocardial and epicardial optical mapping in an acute sheep model. *Circ Arrhythm Electrophysiol* 2015;**8**:456–65.
23. Jacquemet V, Henriquez CS. Genesis of complex fractionated atrial electrograms in zones of slow conduction: a computer model of microfibrosis. *Heart Rhythm* 2009;**6**:803–10.
24. Tanaka K, Zlochiver S, Vikstrom KL, Yamazaki M, Moreno J, Klos M *et al*. Spatial distribution of fibrosis governs fibrillation wave dynamics in the posterior left atrium during heart failure. *Circ Res* 2007;**101**:839–47.
25. Burstein B, Comtois P, Michael G, Nishida K, Villeneuve L, Yeh YH *et al*. Changes in connexin expression and the atrial fibrillation substrate in congestive heart failure. *Circ Res* 2009;**105**:1213–22.
26. Comtois P, Nattel S. Interactions between cardiac fibrosis spatial pattern and ionic remodeling on electrical wave propagation. *ConfProc IEEE Eng Med Biol Soc* 2011:4669–72.
27. Alonso S, Bar M. Reentry near the percolation threshold in a heterogeneous discrete model for cardiac tissue. *Phys Rev Lett* 2013;**110**:158101.
28. Vigmond E, Pashaei A, Cochet H, Amroui S, Haissaguerre M. Percolation as a mechanism to explain atrial fractionated electrograms and reentry in a fibrosis model based on imaging data. *Heart Rhythm* 2016;**13**:1536–43.
29. Wolf RM, Glynn P, Hashemi S, Zarei K, Mitchell CC, Anderson ME *et al*. Atrial fibrillation and sinus node dysfunction in human ankyrin-B syndrome: a computational analysis. *Am J Physiol Heart Circ Physiol* 2013;**304**:H1253–66.
30. Camelliti P, Green CR, LeGrice I, Kohl P. Fibroblast network in rabbit sinoatrial node: structural and functional identification of homogeneous and heterogeneous cell coupling. *Circ Res* 2004;**94**:828–35.
31. Pedrotty DM, Klinger RY, Kirkton RD, Bursac N. Cardiac fibroblast paracrine factors alter impulse conduction and ion channel expression of neonatal rat cardiomyocytes. *Cardiovasc Res* 2009;**83**:688–97.
32. Ashihara T, Haraguchi R, Nakazawa K, Namba T, Ikeda T, Nakazawa Y *et al*. The role of fibroblasts in complex fractionated electrograms during persistent/permanent atrial fibrillation: implications for electrogram-based catheter ablation. *Circ Res* 2012;**110**:275–84.
33. Verheule S, Tuyls E, Gharaviri A, Hulsmans S, van Hunnik A, Kuiper M *et al*. Loss of continuity in the thin epicardial layer because of endomysial fibrosis increases the complexity of atrial fibrillatory conduction. *Circ Arrhythm Electrophysiol* 2013;**6**:202–11.
34. Roney C, Bayer JD, Zahid S, Meo M, Boyle PM, Trayanova NA *et al*. Modelling Methodology of atrial fibrosis affects rotor dynamics and electrograms. *Europace* 2016;**18**(Suppl 4):iv146–55.
35. McDowell KS, Vadakkumpadan F, Blake R, Blauer J, Plank G, MacLeod RS *et al*. Methodology for patient-specific modeling of atrial fibrosis as a substrate for atrial fibrillation. *J Electrocardiol* 2012;**45**:640–5.
36. McDowell KS, Vadakkumpadan F, Blake R, Blauer J, Plank G, Macleod RS *et al*. Mechanistic inquiry into the role of tissue remodeling in fibrotic lesions in human atrial fibrillation. *Biophys J* 2013;**104**:2764–73.
37. Courtemanche M, Ramirez RJ, Nattel S. Ionic mechanisms underlying human atrial action potential properties: insights from a mathematical model. *Am J Physiol* 1998;**275**:H301–21.
38. Krummen DE, Bayer JD, Ho J, Ho G, Smetak MR, Clopton P *et al*. Mechanisms of human atrial fibrillation initiation: clinical and computational studies of repolarization restitution and activation latency. *Circ Arrhythm Electrophysiol* 2012;**5**:1149–59.
39. McDowell KS, Zahid S, Vadakkumpadan F, Blauer J, MacLeod RS, Trayanova NA. Virtual electrophysiological study of atrial fibrillation in fibrotic remodeling. *PLoS One* 2015;**10**:e0117110.
40. Akoum N, Daccarett M, McGann C, Segerson N, Vergara G, Kuppahally S *et al*. Atrial fibrosis helps select the appropriate patient and strategy in catheter ablation of atrial fibrillation: a DE-MRI guided approach. *J Cardiovasc Electrophysiol* 2011;**22**:16–22.
41. Haissaguerre M, Hocini M, Denis A, Shah AJ, Komatsu Y, Yamashita S *et al*. Driver domains in persistent atrial fibrillation. *Circulation* 2014;**130**:530–8.
42. Narayan SM, Krummen DE, Shivkumar K, Clopton P, Rappel WJ, Miller JM. Treatment of atrial fibrillation by the ablation of localized sources: CONFIRM (Conventional Ablation for Atrial Fibrillation With or Without Focal Impulse and Rotor Modulation) trial. *J Am Coll Cardiol* 2012;**60**:628–36.
43. Harrild D, Henriquez C. A computer model of normal conduction in the human atria. *Circ Res* 2000;**87**:E25–36.
44. Zahid S, Cochet H, Boyle PM, Schwarz EL, Whyte KN, Vigmond EJ *et al*. Patient-derived models link reentrant driver localization in atrial fibrillation to fibrosis spatial pattern. *Cardiovasc Res* 2016;**110**:443–54.
45. Boyle PM, Zahid S, Schwarz E, Whyte K, Vigmond EJ, Dubois R *et al*. Prevalence of regions with highly intermingled fibrotic and non-fibrotic tissue is a better

predictor of arrhythmia inducibility than total fibrosis burden: analysis of patient-specific models of persistent atrial fibrillation. *Heart Rhythm* 2015;**12**:S80.
46. Avila G, Medina IM, Jimenez E, Elizondo G, Aguilar CI. Transforming growth factor-beta1 decreases cardiac muscle L-type Ca2+ current and charge movement by acting on the Cav1.2 mRNA. *Am J Physiol Heart Circ Physiol* 2007;**292**:H622–31.
47. Ramos-Mondragon R, Vega AV, Avila G. Long-term modulation of Na+ and K+ channels by TGF-beta1 in neonatal rat cardiac myocytes. *Pflugers Arch* 2011;**461**:235–47.
48. Li D, Fareh S, Leung TK, Nattel S. Promotion of atrial fibrillation by heart failure in dogs: atrial remodeling of a different sort. *Circulation* 1999;**100**:87–95.
49. Platonov PG, Mitrofanova LB, Orshanskaya V, Ho SY. Structural abnormalities in atrial walls are associated with presence and persistency of atrial fibrillation but not with age. *J Am Coll Cardiol* 2011;**58**:2225–32.
50. Chrispin J, Gucuk Ipek E, Zahid S, Prakosa A, Habibi M, Spragg D *et al*. Lack of regional association between atrial late gadolinium enhancement on cardiac magnetic resonance and atrial fibrillation rotors. *Heart Rhythm* 2016;**13**:654–60.
51. Zahid S, Whyte KN, Schwarz EL, Blake RC, Boyle PM, Chrispin J *et al*. Feasibility of using patient-specific models and the minimum cut algorithm to predict optimal ablation targets for left atrial flutter. *Heart Rhythm* 2016;**13**:1687–98.
52. Boykov Y, Kolmogorov V. An experimental comparison of min-cut/max-flow algorithms for energy minimization in vision. *IEEE Trans Pattern Anal Mach Intell* 2004;**26**:1124–37.
53. Bayer JD, Roney CH, Pashaei A, Jais P, Vigmond EJ. Novel radiofrequency ablation strategies for terminating atrial fibrillation in the left atrium: a simulation study. *Front Physiol* 2016;**7**:108.
54. Trayanova NA, Boyle PM. Advances in modeling ventricular arrhythmias: from mechanisms to the clinic. *Wiley Interdiscip Rev Syst Biol Med* 2014;**6**:209–24.
55. Trayanova NA, Boyle PM, Arevalo HJ, Zahid S. Exploring susceptibility to atrial and ventricular arrhythmias resulting from remodeling of the passive electrical properties in the heart: a simulation approach. *Front Physiol* 2014;**5**:435.
56. Ashikaga H, Arevalo H, Vadakkumpadan F, Blake RC III, Bayer JD, Nazarian S *et al*. Feasibility of image-based simulation to estimate ablation target in human ventricular arrhythmia. *Heart Rhythm* 2013;**10**:1109–16.
57. Arevalo HJ, Vadakkumpadan F, Guallar E, Jebb A, Malamas P, Wu KC *et al*. Arrhythmia risk stratification of patients after myocardial infarction using personalized heart models. *Nat Commun* 2016;**7**:11437.
58. Deng D, Arevalo HJ, Prakosa A, Callans D, Trayanova NA. A Feasibility study of arrhythmia risk prediction in patients with myocardial infarction and preserved ejection fraction. *Europace* 2016;**18**(Suppl 4):iv60–6.